# Eccentricity Paces Late Pleistocene Glaciations

**T. Blackburn[1]** , **S. Kodama[1]** , and **G. Piccione[2]**

[1]Earth and Planetary Sciences, University of California Santa Cruz, Santa Cruz, CA, USA, [2]Department of Earth, Environmental, and Planetary Science, Brown University, Providence, RI, USA

**Abstract** Late Pleistocene glacial terminations are caused by rising atmospheric $CO_2$ occurring in response to atmospheric and ocean circulation changes induced by increased discharge from Northern Hemisphere ice sheets. While climate records place glacial terminations coincident with decreasing orbital precession, it remains unclear why a specific precession minimum causes a termination. We compare the orbital and ice volume configuration at each precession minima over the last million years to demonstrate that eccentricity, through its control on precession amplitude, period and coherence with obliquity, along with ice sheet size, determine whether a given precession minimum will cause a termination. We also demonstrate how eccentricity controls obliquity maxima and precession minima coherence, varying the duration of glaciations. Glaciations lasting ~100 thousand years are controlled by Earth's eccentricity cycle of the same period, while the shortest (20–40 ka) and longest (155 ka) occupy the maxima and minimums of the 400 thousand year eccentricity cycle.

**Plain Language Summary** The Milankovitch theory of the ice ages predicts that the growth and collapse of Pleistocene ice sheets is paced by the cycles in high latitude solar insolation that accompany variations in Earth's orbital motion. The orbital modes that dominate frequencies of incoming solar radiation are obliquity and precession, which operate at periodicities of approximately 40 and 20 thousand years, respectively. The dominant frequency at which ice sheets grow and collapse over the last million years is, however, approximately 100 thousand years, a closer match to eccentricity, an orbital period near absent from past solar radiation. Through a comparison between Earth's orbital configuration and an approximation of past global ice volume, we identify that the precession minima that trigger ice sheet collapse occur at distinct configuration of eccentricity and ice sheet size. In most cases terminations occur when precession minima align with obliquity maxima. We find that this coherence is influenced by the duration of precession cycles, which is in turn controlled by eccentricity. From these observations, we conclude that orbital eccentricity, through its control on both the amplitude and period of precession, paces the timing of glacial terminations and the size of Late Pleistocene ice sheets.

## 1. Introduction

The correlation between orbital precession and paleoclimate proxies for polar temperature (Jones et al., 2023; Jouzel et al., 2007), Asian Monsoon intensity (Cheng et al., 2016), global ice volume (Lisiecki & Raymo, 2005) and Northern Hemisphere (NH) ice sheet discharge (Barker et al., 2022) have supported arguments that precession controlled (e.g., Hobart et al., 2023) changes in the solar energy reaching high NH latitudes in summer pace the growth and collapse of late Pleistocene ice sheets (i.e., Milanovich Theory). However, the fact that these changes in radiative forcing are too small to drive the observed shifts in global and polar temperatures (Brook & Buizert, 2018) and that glacial terminations (hereafter terminations) corresponds to a wide range in maximum insolation values (Denton et al., 2010) suggests the absolute value of high latitude NH insolation is, at least over the last million years (Tzedakis et al., 2017), not the lone distinguishing factor in determining whether a termination will occur.

Historically, the most problematic aspect of Milankovitch theory comes from the observation that the cycles in global ice volume, recorded by the composition of benthic foraminifera during the Late Pleistocene (Lisiecki & Raymo, 2005), are dominated by a ~100 thousand year (ka) period, a frequency that is nearly absent from spectral analysis of high latitude summer insolation (Hays et al., 1976; Imbrie et al., 1993). The misalignment between the power spectrum in insolation and global ice volumes, widely referred to as the "100 thousand year problem," has resulted in the incorporation of Milankovitch theory into a hybrid model that includes internal feedbacks (Denton et al., 2010; Lisiecki, 2010), whereby solar energy plays a part in, and is perhaps the trigger to, a sequence of processes that control the collapse of NH ice. The principal among this termination sequence is atmospheric $CO_2$

(Parrenin et al., 2013; Petit et al., 1999) which increases synchronously, within the uncertainties of age models, with changes in polar temperatures (Parrenin et al., 2013). Rapid increases in $CO_2$ that occur during each termination are attributed to $CO_2$ ventilation via upwelling of Southern Ocean bottom waters driven by the southward shift in westerly winds (Ai et al., 2020; Anderson et al., 2009). This shift in wind belts occur as a result of a cooling NH and the weakening of Atlantic Meridional Overturning Circulation (AMOC) (Böhm et al., 2015; Cheng et al., 2016). Weakening of AMOC has been attributed to increased meltwater discharge from the NH, which has been suggested to peak during periods of high NH summer insolation during terminations (Böhm et al., 2015; Denton et al., 2010).

The coincidence of terminations with rising summer insolation in the NH (decreasing precession) has been interpreted to result in glacial cycle durations that are an integer number of precession cycles (Cheng et al., 2016). Rather than a set 100-ka periodicity, glacial-interglacial cycles during the past million years have typically been viewed to vary between 4 and 6 precession cycles (~75 and 120 ka) (Cheng et al., 2016; Hobart et al., 2023). Including terminations recognized at 220 ka (T3a) and 580 ka (T7a) (Cheng et al., 2016)—which are indistinguishable from accepted terminations with respect to the rate of change in global ice volume (Figure 1a) or absolute value of $CO_2$ and polar temperatures (Figure S1 in Supporting Information S1)—reveals that glacial cycles can be as short as 1–2 precession cycles (25 and 41 ka). When examined on a case-by-case basis rather than through an integrated frequency analysis of $\delta^{18}O_{benthic}$ timeseries, it is found that Late Pleistocene glacial cycles are most often ~90 ka in duration (Maslin & Ridgwell, 2005), but can be as short as 20 ka or as long as 155 ka (Figure 1).
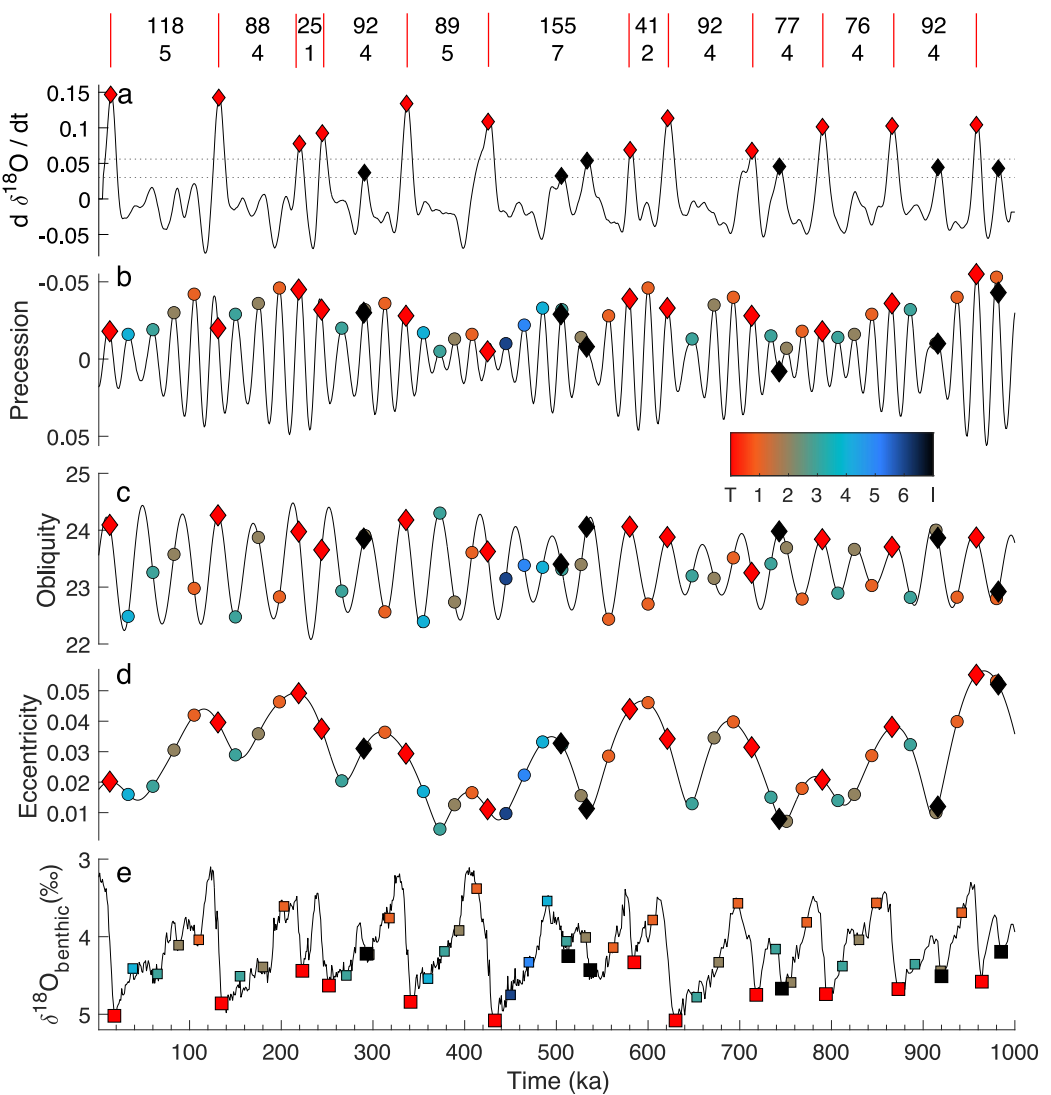
Prior efforts to explain the duration of glacial cycles have independently concluded that precession (Cheng et al., 2016; Hobart et al., 2023), obliquity (Huybers & Wunsch, 2005), eccentricity (Abe-Ouchi et al., 2013; Lisiecki, 2010; Maslin & Ridgwell, 2005), or some combination (Barker et al., 2022; Huybers, 2011) control the pacing of late Pleistocene terminations. In addition to orbital parameters, studies have stressed the importance of ice sheet size in determining whether a termination occurs, specifying the requirement that a large NH ice sheet has accumulated instabilities and is vulnerable to collapse (Abe-Ouchi et al., 2013; MacAyeal, 1979; Maslin & Ridgwell, 2005; Raymo, 1997). We combine these frameworks to show how the orbital configuration required to cause a termination is a function of ice sheet size, which creates the apparently irregular duration in Late Pleistocene glaciations.

## 2. Comparing Ice Sheet Size With Orbital Parameters

Herein we work to understand the interplay between astronomical cycles and ice sheet size in determining when terminations occur. We define glacial cycle durations as the time between terminations and define terminations as times marked by rapid ice loss. Using a sliding derivative of the $\delta^{18}O_{benthic}$ timeseries (Lisiecki & Raymo, 2005) over a 10 thousand year window, we identify 12 events within the last million years characterized by the most rapid ice loss (Figure 1a, red diamonds). This definition excludes the period of ice loss at ~534 ka, which has been defined as a termination (T6) by previous studies (Railsback et al., 2015; Tzedakis et al., 2017). We find this event to be comparable in scale to events at approximately 290, 505, 745 and 920 ka (Figure 1a, black diamonds), which we refer to here as "incomplete" terminations. These events fail to induce the same magnitude of ice loss (Figure 1e), polar temperatures, or atmospheric $CO_2$ concentrations (Figure S1 in Supporting Information S1) as at "successful" terminations. This, as demonstrated below, is the result of the difference in orbital parameters and ice sheet size relative to successful terminations.

Figure 1b presents Earth's climatic precession (hereafter, precession) (Berger & Loutre, 1991, 1999) over the last million years where precession minima are colored by their sequence in a glacial cycle. Red diamonds indicate a "successful" precession cycle that produced a termination (from Figure 1a). Circle markers map the subsequent "failed" precession cycles, (i.e., did not produce a termination) over each glacial period. The increasingly cool colors of these failed precession cycles reflect the increasing number of precession cycles since the last termination.
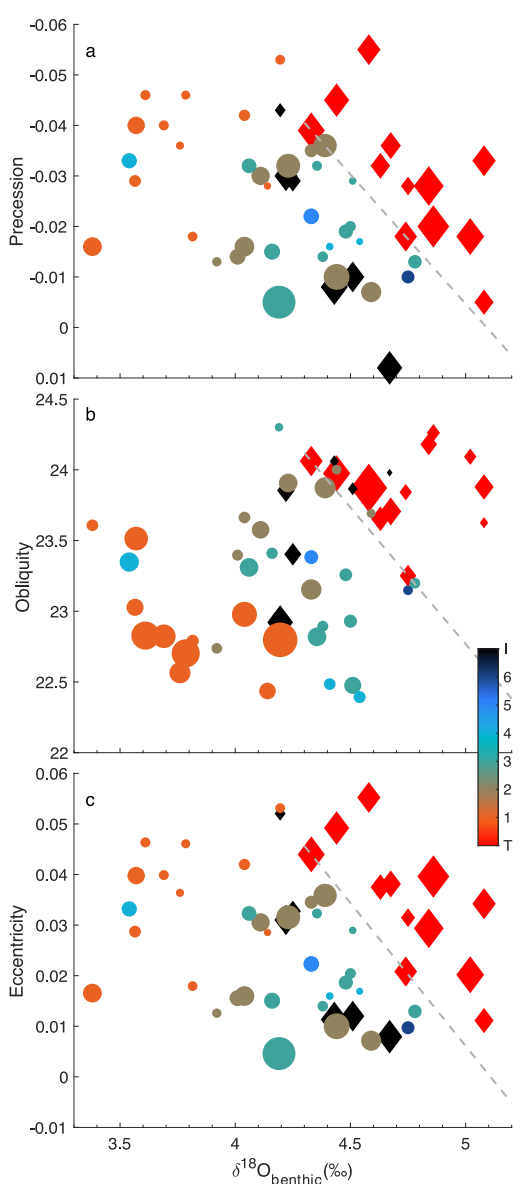
To interrogate why some precession cycles resulted in terminations while others failed, we create a cross-plot of precession at the time of each termination and the corresponding global ice volume ($\delta^{18}O_{benthic}$) that occurred during the glacial maximum prior to the termination (Figure 2a). This lag is used to characterize the ice sheet when it is largest and most vulnerable to collapse. For each precession cycle that failed to result in a termination, we use the precession value at the local minima and the $\delta^{18}O_{benthic}$ value 5 ka prior to the precession minima: a

**Figure 1.** Orbital and paleoclimate time series over the last 1 million years. Glacial duration (ka) and integer of precession cycles noted in the header. (a) The running derivative (10 ka window) of $\delta^{18}O_{benthic}$ record from panel (f) Derivatives that exceed 0.056 $\delta^{18}O$/ka (upper dashed line) are defined as terminations (red diamonds). Derivatives that fall below 0.056 $\delta^{18}O$/ka but above 0.03 0.056 $\delta^{18}O$/ka (lower dashed line) are defined as incomplete terminations (black diamonds). (b) Climatic precession, where red diamonds mark terminations as defined in panel a and circles mark precession minima that did not result in terminations, colored by their sequence in the glaciation (colorbar). Black diamonds mark the incomplete terminations as defined in panel (a) (c) Orbital obliquity and (d) Orbital eccentricity with markers at the times of precession minima from panel (b) (f) $\delta^{18}O_{benthic}$ record (Lisiecki & Raymo, 2005) with markers plotting, for the terminations, the glacial maximum values that precede the terminations and for the remaining markers a value that precedes the precession minima by a comparable lag of 5ka.

value that matches the average time between terminations and glacial maxima. Note that the use of $\delta^{18}O_{benthic}$ as a global ice volume proxy assumes that changes in the $\delta^{18}O_{benthic}$ record over the last 1 million years reflects ice volume alone and that any temperature effects between a glacial and interglacial period are relatively constant from one glacial cycle to the next. The LR04 $\delta^{18}O_{benthic}$ record is also orbitally tuned which could introduce circular reasoning. To test this possibility we reproduce our analysis using a radioisotopically calibrated $\delta^{18}O_{benthic}$ record (Hobart et al., 2023) that extends to ~650 ka, and find identical results (Figure S2 and S3 in Supporting Information S1).

Figure 2a shows a separation of precession cycles into two fields: a failed termination field characterized by positive precession values and/or low global ice volume, and successful termination field characterized by negative precession values and/or higher global ice volumes, each separated by the inequality $Pr \leq$

**Figure 2.** Comparison between orbital parameters and $\delta^{18}O_{benthic}$ proxy for global ice volume. (a) Circles mark precession minima, sized by obliquity and colored, as in Figure 1b, by there by their sequence in each glacial cycle. Terminations are marked as red diamonds and incomplete terminations as black diamonds as defined in Figure 1a. To access maximum ice sheet instability, termination $\delta^{18}O_{benthic}$ values are taken from the preceding glacial maximum. For consistency, $\delta^{18}O_{benthic}$ for the remaining markers are taken from times 5 ka prior. (b) Values of orbital obliquity at the times of precession minima, sized by inverse precession. (c) Values of orbital eccentricity at each precession minima, sized by obliquity. Gray lines denote boundary of the termination (above) and failed termination (below) fields.

$0.05 \cdot \delta^{18}O - 0.26$ (Figure 2a, gray dashed line). No incomplete terminations (black diamonds), and two failed precession cycles (circles) (6%, 2/36) plot above this line. The incomplete terminations marked by black diamonds occupy a space distinct from full terminations (red diamonds). These events, which mostly occur on precession minima and obliquity highs, fail to produce the same response as successful terminations because either the precession index was too high (e.g., weak NH forcing) or ice volume was too low (Figure 2a).

The separation of terminations from failed precession cycles distinguishes terminations as unique with respect to precession and ice volume. The exceptions to these two-fields includes two minima in precession that failed to result in terminations, but plot within the termination field. Although precession and $\delta^{18}O$ alone cannot clearly separate these failed precession cycles, inclusion of obliquity improves the distinction from precession cycles that result in a termination. Marker size in Figure 2a corresponds to the angle of obliquity at the precession minima. One of these failed precession cycles correspond with low obliquity (small markers), supporting the possibility that these periods of low precession did not result in a termination because they did not coincide with a period of high obliquity. The coherence between obliquity maxima and precession minima (OPNH), which would result in warm NH summers, holds true for only eight of the 12 terminations defined here, with exceptions (220, 250, 425 and 715 ka). These events occurred on precession minima when obliquity is relatively low (12%–50% of peak obliquity) suggesting that in some cases, the precession and ice volume configuration alone can provide suitable conditions to produce terminations.

Figure 1c shows orbital obliquity over the last million years, where red diamonds mark terminations, and circles marking the timing of precession minima. Figure 2b, compares the obliquity values at the time of terminations (red diamonds) and precession minima (circle markers) against corresponding $\delta^{18}O_{benthic}$ values. These data again cluster into two fields: one where precession minima correspond with high obliquity and large ice volumes and resulted in terminations, and another where small ice volumes and low obliquity failed to produce terminations. The fields are separated by the inequality $Ob \geq -1.93 \cdot \delta^{18}O + 32.42$ with three incomplete terminations (50%, 3/6) and 3 failed precession cycles (8%, 3/36) falling above this line (Figure 2b). Each of these outliers occurred at relatively high ice volumes (>4.4‰) and high obliquity (>23.2°) but failed to produce a full termination because the precession index was too large (small markers). While terminations most often occur when obliquity is high and precession approaches a minimum, this analysis (and Figure S4 in Supporting Information S1) reveals that several obliquity maxima occur at high ice volume but do not produce terminations. This implies that obliquity does not, by itself or in conjunction with ice volume, determine when terminations occur.

Figure 2c plots the eccentricity at the time of precession minima (Figure 1d) versus the corresponding $\delta^{18}O_{benthic}$ values (Figure 1e). Successful terminations separate from failed precession cycles, with terminations occurring on precession minima characterized by either high eccentricity when ice sheets are relatively small, or low eccentricity when ice sheets are large, following the inequality $Ec \geq -0.06 \cdot \delta^{18} + 0.29$ and $\delta^{18}O \geq 4.3$. The small difference between Figures 2a and 2c are due to terminations often occurring just prior to a precession minima, whereas eccentricity, as the outer envelope of precession, marks a higher value. This overall pattern in Figure 2c is similar to that observed with precession (Figure 2a) with only one incomplete termination (17%, 1/6) and no failed precession cycles (0/36) falling above the inequality line. This pattern illustrates that the orbital forcing required to terminate a glacial cycle changes as a

**Figure 3.** Eccentricities control on the periodicity and coherence of obliquity and precession. (a) *Left*: Inverted precession. *Right*: eccentricity. Vertical lines mark the minima in 100 ka period of eccentricity. (b) Evolutionary fast Fourier Transform (evoFFT, Kodama & Hinnov, 2014; Li et al., 2019) for eccentricity. (c) *Left*: Absolute difference from mean (21 ka) of precession cycle duration. *Right*: Absolute difference from mean (41 ka) of obliquity cycle duration. (d) EvoFFT of mean normalized precession period (panel c left). (e) EvoFFT for obliquity period (Figure S7 in Supporting Information S1). (f) *Left*: Absolute difference from two of ratio of obliquity period and precession period. (f) *Right*: Correlation of obliquity maxima and precession minima (OPNH) (i.e., Northern Hemisphere forcing), where gray shaded areas above/below midline are in/out phase. Red diamonds mark terminations as defined in Figure 1a and Figure S5a in Supporting Information S1. (g) EvoFFT for ratio of obliquity to precession cycle duration (panel f, left). (h) EvoFFT for OPNH correlation (panel f, right).

function of ice sheet size (Abe-Ouchi et al., 2013; MacAyeal, 1979; Raymo, 1997). The observed inverse correlation stems from an ice sheet that is responsive to changes in precession (and not just obliquity). This includes: (a) A requirement that small ice sheets will fail with strong precession forcing at high eccentricity, while larger ice sheets can fail at precession minima when eccentricity is low (Lisiecki, 2010); (b) Precession cycles in between terminations often occur on the descending limb of a 100 ka eccentricity cycle such that ice volumes are permitted to expand with each lower amplitude precession cycle.

## 2.1. Eccentricity Controls Duration of Glaciations and Ice Volumes

Our analysis clarifies what role each orbital parameter plays in a termination. Terminations occur on a precession minima, where the index required to induce failure scales with ice sheet volume, and often with OPNH coherence. Here we describe 3 mechanisms by which eccentricity modulates these orbital parameters and paces Pleistocene glaciations:

1. Eccentricity's modulation of precession's amplitude (Figure 3a). The precession of Earth's rotation axis leads to larger and smaller contrast in seasonal insolation values. A negative precession index results in stronger NH Summer Insolation (NHSI). The eccentricity of Earth's orbit modulates this effect, where low eccentricity orbits reduce seasonal contrasts caused by precession (and vice versa) causing variations in precession minima that approach 200%.
2. Eccentricity's control on precession and obliquity period duration, and therefore precession and obliquity coherence. Over the Pleistocene, the mean precession period duration is ~21 ka (Figure S7 in Supporting Information S1). However, the duration of precession cycles can vary from 10 to 30 ka at the eccentricity

minima (nodes) associated with the ∼100 ka periodicity in eccentricity (Huybers & Aharonson, 2010). We report deviations in precession period from the mean (Figure 3c), which shows a consistent ∼100 ka periodicity (Figure 3d). Obliquity period experiences smaller scale variations (∼20%), however these are also controlled by eccentricity as predicted by Equation 2 in Laskar and Robutel (1993) where the change in obliquity (and precession) depends on the eccentricity (*e*), in the $(1-e^2)^{-3/2}$ term. This relationship between obliquity and eccentricity is supported by the ∼100 ka periodicity seen in the evolutionary fast Fourier transform for obliquity period (Figure 3e) as well as a correlation between obliquity period and amplitude (Figure S8 in Supporting Information S1) and a shared periodicity (2.4 Ma) between obliquity amplitude and eccentricity (Figure S9 in Supporting Information S1).
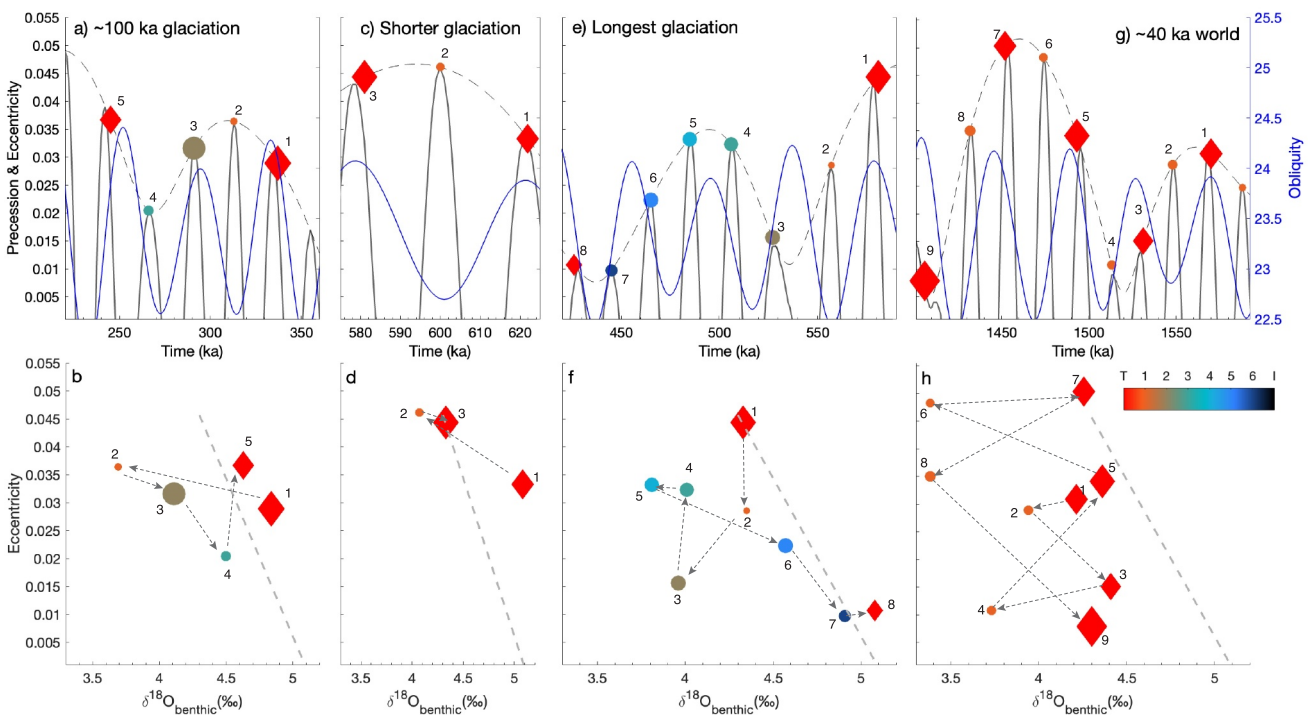
Since the period duration of precession and obliquity vary, their coherence in producing warm NH summers will also vary. To determine the degree and timing of precession and obliquity coherence for producing warm NH summers, we calculate a running correlation (abbreviated as OPNH) between obliquity greater than the mean (23.3°) and precession less than zero (Figure S10 in Supporting Information S1) (Cooper & Cowan, 2008). Figure 3f (gray shading) shows prolonged periods of in-phase (above midline) and out of phase (below midline) coherence. Periods of coherence correspond to times when the leads/lags between OPNH are smallest and periods of non-coherence correspond to times when the leads/lags are largest (Figure S10c in Supporting Information S1). Both results demonstrate that OPNH phasing alternates between times of fully in/out of phase coherence (Figure 3f) with a periodicity of 200–250 ka (Figure 3h).

We propose that the mechanism driving OPNH coherence cycles is changes in precession and obliquity period durations (Figure 3c). The mean period durations of obliquity (41 ka) and precession (21 ka) have a ratio of ∼2, which creates a constant phase relation. When the ratio of their period durations deviates from 2, these phases shift relative to each other. Since changes in precession period duration are relatively larger than obliquity, deviations in the ratio between O-P period durations, and resulting phase shifts, are primarily caused by changes in precession period duration. Precession period duration changes most at the 100 ka nodes of eccentricity (vertical lines, Figure 3), resulting in a phase shift of precession and obliquity every ∼100 ka (Figure 3f). The ∼200–250 ka periodicity in OPNH coherence at these times (Figure 3h) is approximately double the ∼100 ka eccentricity cycle: one eccentricity node turns OPNH phasing on, the next node turns it off and a third turns OPNH back on again: 2 full ∼100ka eccentricity periods are required to complete an OPNH cycle. Due to the prevalence of OPNH phasing associated with terminations, we posit that the loss of OPNH phasing prolongs glacial periods by preventing terminations from occurring. Deviations from this 200−250 ka periodicity are discussed in the next section.

3. Secular variations in eccentricity. The relative power of Earth's 100 and 400 ka eccentricity cycles varies over a 2,400 ka period (Figure 3b). These secular variations effect the pacing of glaciations through their influence on the above mechanisms. For example, the strengthening of the 400-ka periodicity in the latest Pleistocene (Figure 3b) decreases the amplitude of precession favoring ice accumulation. A less obvious example relates to deviations from the ∼200–250 ka periodicity in OPNH coherence. Over the last 2,500 ka, there are two relatively long (∼400 ka) time periods centered at ∼950 and 1,800 ka (Figures 3f and 3h) where the 200–250 periodicity in OPNH is lost and OPNH is neither fully in nor out of phase. These periods coincide with the transitions between the relative power between the 100 and 400 ka periodicities in eccentricity (Figure 3b), a trend that continues back to 5 Ma (Figure S11 in Supporting Information S1). How the 2.4 Ma eccentricity cycle controls OPNH and influences glaciations remains to be understood, however we propose that this behavior relates to a larger range in the obliquity period at these transitional time periods (Figure 3e; Figure S11 in Supporting Information S1) and that OPNH through these intervals, which includes the Mid Pleistocene Transition, may influence the periodicity of glaciations.

## 2.2. Eccentricity Controls in Practice

Of the 11 glaciations over the last million years, the duration of six are controlled by the 100 ka periodicity of eccentricity modulating precession. These glaciations lasting four precession cycles begin with terminations occurring when precession and obliquity are coherent near a 100 ka maximum in eccentricity (Figure 4a). The next precession cycle is skipped because this cycle occurs out of phase of obliquity and the ice sheet volume is still small. Declining eccentricity over the duration of the second and third precession cycles favors ice sheet growth (Abe-Ouchi et al., 2013). The glacial cycle terminates on the fourth precession cycle when eccentricity (and therefore precession index) increases due to the 100 ka cycle. This increase in insolation, paired with a large ice

**Figure 4.** Illustration of orbital controls on (a–b). ~100 ka glaciations; (c–d). Shorter glaciations (e–f). Longer Glaciations and (g–h). ~40 ka Early Pleistocene glaciations. Red diamonds mark terminations. Circle markers are precession minima colored as in Figures 2 and 3 (color bar). Numbers mark precession cycles. Markers size set by orbital obliquity. (a, c, e, g) Inverse precession and eccentricity are plotted on the left side axis and obliquity on the right side of the time series. (b, d, f, h) Eccentricity is plotted on the *y*-axis in comparison to $\delta^{18}$O. Gray lines denote boundary of the termination (above) and failed termination (below) fields defined in Figure 2c.

sheet, leads to ice sheet collapse (Figure 4b). The absolute duration of the six glaciations that follow this sequence varies between 77 and 92 ka (Figure 1, heading), and is the result of eccentricities modulation of precession period.

The shortest glaciations occupy the maximum amplitudes of the 400 ka periodicity of eccentricity. At ~600 ka (Figure 4c), the constructive coherence of precession, obliquity, and both the 100 and 400 ka eccentricity cycles results in maximum NH summer warming, sufficient to trigger collapse of a relatively small ice sheet ($\delta^{18}$O ~4.3‰, Figure 4d) after just two precession cycles. A similar orbital configuration results in a shorter glacial cycle at ~250 ka, that lasts only one precession cycle (Cheng et al., 2016).

The longest glaciation and largest ice sheet of the late Pleistocene occupy the minimums of the 400 ka periodicity of eccentricity (Figure 4e). The reduced eccentricity (and therefore precession amplitude) favors ice sheet growth over ablation. An eccentricity minima at ~540 ka produced a switch to lost OPNH coherence across most of the longest glaciation (~425–580 ka, Figure 3f). The net effect of dampened precession amplitude and loss of OPNH is cooler NH summers permitting both a skipped 100 ka eccentricity cycle and the longest glaciation (155 ka) that resulted in the largest ice sheet ($\delta^{18}$O ~5.1‰, Figure 4f) over the last million years.

This sensitivity to precession in the Late Pleistocene is in contrast to the ice sheets of the Early Pleistocene, where terminations do occur at precession minima and obliquity maxima (Barker et al., 2022) (Figures 4g and 4h; Figure S5 in Supporting Information S1), but over the entire range of precession minima (Figure S6 in Supporting Information S1). The increased response to precession in the Late Pliestocene, suggests that ice sheets expanded to lower latitudes (Barker et al., 2022), an observation that implies that the increase in $\delta^{18}$O across the Mid-Pleistocene transition is at least in part the result of ice expansion to lower latitudes.

## 3. Conclusion

Our analysis illustrates the role that each orbital parameter plays in producing Late Pleistocene terminations while highlighting the key role of eccentricity, through its control on the amplitude and period of precession, in pacing these events. A comparison between the global ice volume and Earth's orbital configuration at each precession cycle over the last million years, reveals that the timing of glacial terminations are dictated by ice sheet size and precession. While these events most often occur when precession minima align with obliquity maxima, it is the large variation in the amplitude of precession, modulated by eccentricity, that produces the irregular time pacing of Late Pleistocene terminations. Additionally, eccentricity controls the phasing between obliquity and precession through its influence on the duration of obliquity and precession periods, the latter of which can vary widely at the minima of the 100 ka eccentricity cycle. Thus the alignment of OPNH, such that the NH experiences intense summer warming at every other precession minima, cycles on/off with the 100 ka eccentricity cycle. Over the last million years, terminations tend to occur on the rising arm of Earth's 100 thousand year periodicity in eccentricity, resulting in glaciations of similar duration. The shortest (20 ka) occur at the lowest precession index on the maxima of the 400 thousand year eccentricity cycle. The longest glaciation (155 ka) occupies a minima of the 400 thousand year eccentricity cycle, but also overlaps with a period of lost OP phasing, the result of which is a 100 ka eccentricity cycle with no termination and the largest ice sheet of the Late Pleistocene.

## Conflict of Interest

The authors declare no conflicts of interest relevant to this study.

## Data Availability Statement

The data used in this paper includes (Berger & Loutre, 1991; Lisiecki & Raymo, 2005) and software from Li et al. (2019).

## References

Abe-Ouchi, A., Saito, F., Kawamura, K., Raymo, M. E., Okuno, J. i., Takahashi, K., & Blatter, H. (2013). Insolation-driven 100,000-year glacial cycles and hysteresis of ice-sheet volume. *Nature*, *500*(7461), 190–193. https://doi.org/10.1038/nature12374

Ai, X. E., Studer, A. S., Sigman, D. M., Martínez-García, A., Fripiat, F., Thöle, L. M., et al. (2020). Southern Ocean upwelling, Earth's obliquity, and glacial-interglacial atmospheric CO2 change. *Science*, *370*(6522), 1348–1352. https://doi.org/10.1126/science.abd2115

Anderson, R. F., Ali, S., Bradtmiller, L. I., Nielsen, S. H. H., Fleisher, M. Q., Anderson, B. E., & Burckle, L. H. (2009). Wind-driven upwelling in the Southern Ocean and the deglacial rise in atmospheric CO2. *Science*, *323*(5920), 1443–1448. https://doi.org/10.1126/science.1167441

Barker, S., Starr, A., van der Lubbe, J., Doughty, A., Knorr, G., Conn, S., et al. (2022). Persistent influence of precession on northern ice sheet variability since the early Pleistocene. *Science*, *376*(6596), 961–967. https://doi.org/10.1126/science.abm4033

Berger, A., & Loutre, M.-F. (1991). Insolation values for the climate of the last 10 million years [Dataset]. *Quaternary Science Reviews*, *10*(4), 297–317. https://doi.org/10.1016/0277-3791(91)90033-Q

Berger, A., & Loutre, M.-F. (1999). Parameters of the Earths orbit for the last 5 Million years in 1 kyr resolution [Dataset]. *PANGAEA*. https://doi.org/10.1594/PANGAEA.56040

Böhm, E., Lippold, J., Gutjahr, M., Frank, M., Blaser, P., Antz, B., et al. (2015). Strong and deep Atlantic meridional overturning circulation during the last glacial cycle. *Nature*, *517*(7532), 73–76. https://doi.org/10.1038/nature14059

Brook, E. J., & Buizert, C. (2018). Antarctic and global climate history viewed from ice cores. *Nature*, *558*(7709), 200–208. https://doi.org/10.1038/s41586-018-0172-5

Cheng, H., Edwards, R. L., Sinha, A., Spötl, C., Yi, L., Chen, S., et al. (2016). The Asian monsoon over the past 640,000 years and ice age terminations. *Nature*, *534*(7609), 640–646. https://doi.org/10.1038/nature18591

Cooper, G. R. J., & Cowan, D. R. (2008). Comparing time series using wavelet-based semblance analysis. *Computers and Geosciences*, *34*(2), 95–102. https://doi.org/10.1016/j.cageo.2007.03.009

Denton, G. H., Anderson, R. F., Toggweiler, J. R., Edwards, R. L., Schaefer, J. M., & Putnam, A. E. (2010). The last glacial termination. *Science*, *328*(5986), 1652–1656. https://doi.org/10.1126/science.1184119

Hays, J. D., Imbrie, J., & Shackleton, N. J. (1976). Variations in the Earth's Orbit: Pacemaker of the Ice Ages: For 500,000 years, major climatic changes have followed variations in obliquity and precession. *Science*, *194*(4270), 1121–1132. https://doi.org/10.1126/science.194.4270.1121

Hobart, B., Lisiecki, L. E., Rand, D., Lee, T., & Lawrence, C. E. (2023). Late Pleistocene 100-kyr glacial cycles paced by precession forcing of summer insolation. *Nature Geoscience*, *16*(8), 717–722. https://doi.org/10.1038/s41561-023-01235-x

Huybers, P. (2011). Combined obliquity and precession pacing of late Pleistocene deglaciations. *Nature*, *480*(7376), 229–232. https://doi.org/10.1038/nature10626

Huybers, P., & Aharonson, O. (2010). Orbital tuning, eccentricity, and the frequency modulation of climatic precession. *Paleoceanography*, *25*(4). https://doi.org/10.1029/2010pa001952

Huybers, P., & Wunsch, C. (2005). Obliquity pacing of the late Pleistocene glacial terminations. *Nature*, *434*(7032), 491–494. https://doi.org/10.1038/nature03401

Imbrie, J., Berger, A., Boyle, E. A., Clemens, S. C., Duffy, A., Howard, W. R., et al. (1993). On the structure and origin of major glaciation cycles 2. The 100,000-year cycle. *Paleoceanography*, *8*(6), 699–735. https://doi.org/10.1029/93pa02751

Jones, T. R., Cuffey, K. M., Roberts, W. H. G., Markle, B. R., Steig, E. J., Stevens, C. M., et al. (2023). Seasonal temperatures in west Antarctica during the holocene. *Nature*, *613*(7943), 292–297. https://doi.org/10.1038/s41586-022-05411-8

Jouzel, J., Masson-Delmotte, V., Cattani, O., Dreyfus, G., Falourd, S., Hoffmann, G., et al. (2007). Orbital and millennial Antarctic climate variability over the past 800,000 years. *Science*, *317*(5839), 793–796. https://doi.org/10.1126/science.1141038

Kodama, K. P., & Hinnov, L. A. (2014). *Rock magnetic cyclostratigraphy* (Vol. 5). John Wiley and Sons. https://doi.org/10.1002/9781118561294

Laskar, J., & Robutel, P. (1993). The chaotic obliquity of the planets. *Nature*, *361*(6413), 608–612. https://doi.org/10.1038/361608a0

Li, M., Hinnov, L., & Kump, L. (2019). *Acycle*: Time-series analysis software for paleoclimate research and education [Software]. *Computers and Geosciences*, *127*, 12–22. https://doi.org/10.1016/j.cageo.2019.02.011

Lisiecki, L. E. (2010). Links between eccentricity forcing and the 100,000-year glacial cycle. *Nature Geoscience*, *3*(5), 349–352. https://doi.org/10.1038/ngeo828

Lisiecki, L. E., & Raymo, M. E. (2005). A Pliocene-Pleistocene stack of 57 globally distributed benthic δ18O records [Dataset]. *Paleoceanography*, *20*(1). https://doi.org/10.1594/PANGAEA.704257

MacAyeal, D. R. (1979). A catastrophe model of the paleoglimate. *Journal of Glaciology*, *24*(90), 245–257. https://doi.org/10.3189/s0022143000014775

Maslin, M. A., & Ridgwell, A. J. (2005). Mid-Pleistocene revolution and the 'eccentricity myth'. *Geological Society, London, Special Publications*, *247*(1), 19–34. https://doi.org/10.1144/gsl.sp.2005.247.01.02

Parrenin, F., Masson-Delmotte, V., Köhler, P., Raynaud, D., Paillard, D., Schwander, J., et al. (2013). Synchronous change of atmospheric CO2 and Antarctic temperature during the last deglacial warming. *Science*, *339*(6123), 1060–1063. https://doi.org/10.1126/science.1226368

Petit, J.-R., Jouzel, J., Raynaud, D., Barkov, N. I., Barnola, J. M., Basile, I., et al. (1999). Climate and atmospheric history of the past 420,000 years from the Vostok ice core, Antarctica. *Nature*, *399*(6735), 429–436. https://doi.org/10.1038/20859

Railsback, L. B., Gibbard, P. L., Head, M. J., Voarintsoa, N. R. G., & Toucanne, S. (2015). An optimized scheme of lettered marine isotope substages for the last 1.0 million years, and the climatostratigraphic nature of isotope stages and substages. *Quaternary Science Reviews*, *111*, 94–106. https://doi.org/10.1016/j.quascirev.2015.01.012

Raymo, M. E. (1997). The timing of major climate terminations. *Paleoceanography*, *12*(4), 577–585. https://doi.org/10.1029/97pa01169

Tzedakis, P. C., Crucifix, M., Mitsui, T., & Wolff, E. W. (2017). A simple rule to determine which insolation cycles lead to interglacials. *Nature*, *542*(7642), 427–432. https://doi.org/10.1038/nature21364